Final Report

Contract Number:

DACA 3991MO854

Title:

Detection of Shallow Tunnels Emplaced in Unconsolidated Sediments

Submitted to:

U. S. Army Corps of Engineers
Waterways Experiment Station
Geotechnical Laboratory - Geophysics (GL-2)

By:

Dr. Richard D. Rechtien
Geophysical Consultant
Box 78 Route 2
Rolla, Missouri 65401
(314) 341-4665:

Date of Submission:

January 30, 1992

INTRODUCTION

In the summer of 1986 a serious effort to develop seismic instrumentation for the detection of clandestine underground tunnels was initiated by the U.S. Army Belvoir Research, Development and Engineering Center, Ft. Belvoir, VA, under the direction of Mr. Ray Dennis, and by USAE Waterways Experiment Station, Vicksburg, MS, under the direction of Mr. Bob Ballard. Following an extensive period of system development and proof of concept testing, the system was finally accepted by the U.S. Eighth Army and deployed in the Republic of Korea in the summer of 1990.

During the testing stages of the instrument over known tunnels in the Republic of Korea considerable experience was acquired relative to the identification of the seismic signature of a tunnel. While tunnels in Korea are found in hard rock, the experience of discovering what can and cannot be seen by seismic energy probes, as viewed from the perspective of small tunnel targets, nevertheless can be readily applied to other types of host earth materials as well. Consequently, when a tunnel, reportedly used for the smuggling of drugs, was discovered under the U.S.-Mexico border in Douglas, AZ in the summer of 1989 by the U.S. Customs Service, an investigation was launched with the aim of adapting the tunnel experience of Korea to the problem of tunnel detection along the U.S.-Mexican border.

TUNNEL CHARACTERISTICS

The tunnel which was discovered in Douglas, AZ was concrete-lined, approximately 300 ft in length, and was buried approximately 45 ft below the ground surface within a sediment know as caliche. The tunnel itself is about 4 ft wide

and 5 ft high. The roof of the tunnel is arched, or hemi-cylindrical. The thickness of the liner is not known, nor whether it was poured in place or formed with pre-fabricated concrete sections.

This tunnel is located partially beneath an industrial area of Douglas, AZ, and an industrial/residential area of Agua Prieta, Mexico. The vertical plane of the U.S.-Mexican border divides the tunnel into two equal cylindrical parts. The tunnel on the north side of the border passes below a wide drainage ditch that dips at least 10 ft below ground level. Otherwise, the surface of the ground on the north side of the border is covered by industrial construction, streets, parking lots, etc..

PROBLEM AREAS AND METHODS OF APPROACH

The methodology of detection was constrained by requirements from the Drug Enforcement Agency (DEA); the resulting technique was to employ surface instrumentation only, with minimum field visibility. Consequently, the conceivable seismic methods of approach fall within the following application possibilities:

I. Wave field scattering by illumination of the tunnel with a primary, down going energy field created by a P or SH surface energy source.

II. Wave field scattering by illumination of the tunnel with an up going P or SH refraction from a rock interface below the tunnel.

III. Wave field scattering by illumination of the tunnel with a deep penetrating Rayleigh or Love wave.

It is difficult, perhaps impossible, to conceive of a seismic method of tunnel detection that does not center on a

scatter, tunnel-wave interference phenomenon. Any such scattered process is plagued by the reality that such interactions create scattered fields that are rather weak as compared to the energy of illumination. The strength of the scattered field is typically 5, and rarely up to 20, percent of the illumination field. The scattered field strength depends on the ratio of size of the scattering object to energy wavelength, as well as impedance contrast between the object and it's host.

In Category I above, where primary P or SH waves are chosen for the energy probe, the source to receiver offset must be large in order for the scattered field to arrive at times significantly prior to the arrival of the surface waves. The large offset results in two severe disadvantages. First, significant attenuation of the direct wave, due to spherical spreading and material dissipation, will seriously deplete the primary field strength available for tunnel illumination. In particular, the higher frequencies and shorter wavelengths required for visibility of small scattering objects will be lost. Secondly, the principal angle of incidence of the illumination field will be rather shallow, resulting in a scattered field which has it primary radiation lobes oriented, more or less, horizontally. The scattered energy that ultimately reaches the surface over the tunnel will originate from regions near the anti-nodes of the radiation pattern. Consequently, the scattered energy will be very, very weak as compared to the normal activity of direct and refracted waves arriving at about the same time.

In addition to the listed disadvantages of using primary energy waves for the detection of tunnels, there is one very good reason for the selection of an alternate exploration procedure: in the collective history of tunnel detection research the back-scattered, or side-scattered, energy from a tunnel has never been observed. One should not conclude that it does not exist, but only that it is too weak (for scattering objects small relative to wavelength of the energy of

illumination) to be observed.

Wave field scattering by illumination of the tunnel with up-going P or SH refracted wave, as listed in Category II above, would generate a primary scattered energy lobe that was oriented in the upward direction of the refracted field. The interference of this scattered energy with the refracted field would result in a process that has been consistently observed in crosshole studies involving tunnels. One should expect a small time delay of the total field (refracted plus scattered) arriving at the free surface at sensor positions within the shadow zone of the tunnel, together with an amplitude attenuation. Again, however, long offsets of source to receiver would be required since the refractions from deeper layers, which may not be first arrivals, must be separated in time from the arrival of surface wave energy.

A wavelength advantage, by a factor of approximately two, is gained by the deployment of SH waves as opposed to P waves, given the equivalence of energy spectral content. Moreover, the orientation of SH motion parallel to the tunnel axis allows for total conversion of incident energy to SH scattered energy. Consequently, it would be preferable to employ SH energy sources for a refraction approach.

Surface waves, as listed in Category III, are perhaps the most promising seismic energy probe for the detection of shallow, concrete-lined tunnels buried in unconsolidated sediments. As an illustration of the interaction of a tunnel with a surface wave I offer the following results of a 'generic' computer simulation.

Figure 1a illustrates the simple model configuration. Basically, a tunnel is buried in a soil layer above bedrock. A Love wave is assumed to be moving to the right and interacts with the tunnel upon approach. A system of seismometers are located on the air-soil boundary and records the passage of the Love wave and the scattered field. The resulting seismogram

is illustrated in Figure 1b. These data were calculated using a finite-difference computer modelling algorithm of the inhomogeneous, SH, elastic, two-dimensional wave equation. Referencing Figure 1b, times and distances are normalized. The seismic traces are, however, aligned with the seismometer positions as shown in Figure 1a.

The Love arrival in Figure 1b is separated in time from the diffracted, or scattered, field. The amplitude of the diffraction is about 10% of the strength of the Love wave. This event is displaced by a time Δt below the Love wave arrival; the displacement being determined by the ratio of depth of burial to wavelength (D/λ). As D/λ decreases the diffraction arrival will move closer in time to the Love wave arrival, and the initial motion of the diffraction will constructively or destructively interfere with the final motion of the Love wave. Notice that both the Love wave and diffraction arrival will have approximately the same asymptote for large distances from the tunnel. Consequently, when the two events significantly overlap a distortion of the Love wave arrival in the lateral vicinity of tunnel can be expected.

Figure 2 illustrates the passage of the Love wave and subsequent "pealing off" of the diffracted event from the tunnel. Eight progressive time "snapshots" are illustrated, each showing the contours of the absolute value of the particle velocity at that given instant. The wavelength of the Love wave is, here, approximately equal to one-half the tunnel depth, $D/\lambda = 2$. Consequently, in this generic illustration, the diffracted event never reaches the surface in time to interfere with the tail of the Love wave.

Similar illustrations could be presented for Rayleigh waves. But here again, the slowness of the Love wave gives rise to shorter wavelengths; a distinct detection advantage. Consequently, in view of all considerations, the Love wave was chosen as the primary exploration energy probe for this tunnel

scattering problem. Although it is the primary focus of this investigation, field data was examined for the presence of scattered events associated with direct and refracted P and S waves, and Rayleigh wave energies.

THE EXPERIMENT

Test site

A site located within the city limits of Cape Girardeau, MO was chosen for the experiment. As a simulation of a concrete-lined tunnel, a sewer line, buried in deep soil, was chosen as an exploration target. This 30 inch ID line was installed by trenching in the summer of 1991. It is located 20 ft below ground level at the chosen site, and 4 ft above competent bedrock.

The site at Cape Girardeau offers, in some ways, a severer test environment than the site at Douglas. First, the target diameter is smaller by a factor of 2. Thus, wave frequency requirements for detection will increase by a factor of 2 at Cape Girardeau. Secondly, the Cape Girardeau site has been disturbed by trenching, which could introduce local velocity variations in the soil above the target. Thirdly, the soil at Cape Girardeau has significantly less rigidity than caliche and should prove to be a much higher attenuative medium. Lastly, as illuminated by the refraction data acquired at the site, the sewer line was buried within a relatively deep depression of bedrock, which is probably an ancient stream channel. Consequently, in light of the environmental severity, if the test at Cape Girardeau was at all successful relative to target detection, then one could conclude that proof of concept had been established.

Seismic Sources

Compressional waves, used for the purpose of obtaining

bedrock definition, were generated by hammer blows upon a steel plate. This source was also used to investigate Rayleigh waves. For shear waves, a hammer blow against the steel-capped end of a weighted, wooden, horizontal beam was used for SH refraction data. For the study of primary SH and Love wave scattering a source named "The Wacker" was developed and deployed.

The Wacker is shown schematically in Figure 3a. The system consists of a double-headed hammer that rotates horizontally, striking anvils that are rigidly attached to the main housing. The 16 lb hammer heads on either end of the 17 inch rotational arm are accelerated from rest by a 24 volt starting motor. This motor is controlled by relays to limit the duration of current flow to the field and armature, thus allowing control of the impact force supplied by the hammers and the degree of reverse travel after impact due to hammer head rebound. Other relays reverse the rotational direction of the motor to allow for an impact with reversed polarity.

The Wacker has a 36 inch-diameter base and weighs approximately 500 lbs. The base has a pattern of conical earth spikes, 3 inches in length, which produce excellent coupling into soft ground. The system is mounted on an International Scout, as illustrated in Figure 3b, by means of a hydraulic system. As the Wacker is lowered, the hydraulic system pulls the Scout backwards as the spikes begins to dig into the earth, thus placing a portion of the weight of the Scout directly onto the main Wacker housing. A photograph of the deployed system is shown in Figure 4.

The Wacker produces a highly repeatable SH wave field that has horizontally polarized motion. This motion is tangent to expanding cylindrical surfaces, at least in the near field. In addition to better repeatability, the system produces higher frequencies and considerably more energy than manual hammer blows upon the end of a steel-capped, weighted beam.

Sensors and Recording System

For P-wave sources 100 Hz vertically sensitive geophones were used for the sampling of the wave fields. For SH studies 4 Hz horizontally sensitive geophones were employed due to non-availability of higher frequency instrumentation.

A Bison 8012A Engineering Seismograph was used for field recording. The acquired data was later transferred to a Masscomp 5400 computer for analysis and display.

Test Configuration

The test configuration is shown in Figure 5a. P and SH refraction data was used, via the Generalized Reciprocal Method (GRM), to construct the geometry of the subsurface. A shallow interface, at a depth of approximately 4 feet, separates two soil layers having SH velocities of 390 and 1,225 feet per second. A deeper interface between the higher speed soil and bedrock exists at a depth of about 11 feet on one side of the profile and ends up at about 20 feet in depth on the other side. In between these profile extremities bedrock dips sharply to depths which could not be derived from the refraction data. However, bedrock is most certainly located 4 feet or more below the bottom of the sewer line. SH bedrock velocity was found to be 3,900 feet per second.

Data Acquisition

The basic source-sensor configuration used for SH studies is shown in Figure 5a. A constant offset of 20 feet between source and the first receiver (near offset) was employed. Sensor spacing was held fixed at 2 feet. Beginning with the 12th sensor (far offset) located at a surface position

directly above the sewer line, the spread was marched at two foot intervals between data acquisition cycles until the first sensor (near offset) was at the surface position directly over the sewer line. Thus 12 seismograms formed the data base of the SH wave investigation.

A variety of other source-sensor configurations were employed to obtain refraction and Rayleigh wave data. Refraction data was acquired with configurations compatible with GRM.

RESULTS

P-SV and Rayleigh Waves

The experimental P-source data was scanned for any indication of refracted P and Rayleigh wave interactions with the sewer line. Refractions from bedrock below the sewer line were not observed; due, most likely, to the complexity of bedrock geometry. Observed Rayleigh waves had velocities of propagation in the range of 380 to 420 feet per second, which is close to the shear velocity of the low-speed surface layer. The dominant frequency of the Rayleigh wave was 98 Hz, yielding a wavelength in the neighborhood of 4 feet. The root of the Rayleigh wave, consequently, did not significantly penetrate the medium at depth and did not interact with the sewer line. Deeper penetrating Rayleigh waves were not observed.

The P-SV part of this investigation essentially contributed refraction information which led to a better definition of subsurface conditions. Information relative to the interaction of wave energy with the sewer line was not observed in these data.

SH and Love Waves

A typical SH seismogram is shown in Figure 5b. The

source and sensor positions for this record are shown in Figure 5a. The first arrival was a SH refraction from the soil-soil interface residing at a depth of about 4 feet. Since the refracting layer is above the target, no indication of a wave-sewer line interaction should, nor was, observed in this arrival. Refractions from the deeper, soil-rock interface were not observed.

The second major arrival was a Love wave travelling at a speed of 453 feet per second. The dominant frequency of this event was 40 Hz, giving rise to a dominant wavelength of 11 feet. This Love wave-sewer line configuration is comparable to that of the genetic illustration of Figure 2; the ratio of depth to wavelength being about 2 as it was in that simulation. Consequently, one might expect a very weak interaction showing up in a region of the data following the passage of this Love wave. However, other energies occur in the wake of the Love event, having more than sufficient strength to obliterate a weak scattering arrival.

A third major event is marked at an arrival time in the neighborhood of 0.2 sec. This deeper penetrating Love wave travels with a speed of 1,466 feet per second. While the dominant frequency of this event is also around 40 Hz, the dominant wavelength is 37 feet. For this wave the sewer line is located at a depth position of one-half wavelength ($D/\lambda=.5$), placing the pipe within a region of high Love wave energy. Significant scattered energy should, therefore, be expected. Moreover, the scatterer is close enough to the surface, relative to wavelength, to allow for overlapping of the trailing edge of the Love wavelet with the leading edge of the scattered SH wavelet. This interaction should be observable, especially since the region of their occurrence in the record is relatively "quiet".

This record is plotted with true relative amplitude from trace to trace. Upon examination of the leading portion of this Love wave one finds that the wavelet amplitude is relatively

uniform across the record. The trailing portion of the Love wave, however, shows a strong amplitude attenuation. This attenuation is quantified in Figure 6. For sensors close to the vertical plane passing through the centerline of the pipe the signals are attenuated up to 8 dB. The travel time curve for this phase of the Love wave, as shown in Figure 6, does not show any anomalous time delays. This result, together with uniformity of amplitude of the leading edge of the Love wave, leads to the conclusion that trenching did not have a significant influence on the velocity and attenuation structure of the site, except, perhaps, at very shallow depths. Additional attenuation data of the Love wave event for different positions of the source are shown in Figure 7. These data show an amplitude attenuation of the trailing edge of the Love wavelet up to 11 dB.

A trace of the SH scattered (diffracted) wave can also be seen in Figure 5b. This event is, ideally, a cylindrical wave travelling at the speed of the host medium (1,225 feet per second). While this event is small compared to the Love wave amplitude, it can nevertheless be identified.

DISCUSSION AND CONCLUSIONS

The results of this experiment are consistent with prior tunnel research and are about at the level of expectation. The interaction of the sewer line with the deeper penetrating Love wave offers a promising procedure for the detection of shallow tunnels. The arrival time of this interaction takes place in the record after multi-path, early arriving energy activity has settled down to reasonable levels. This second Love wave is quite distinct and set apart from the slower moving, shallow penetrating event; a behavior which is not observed for Rayleigh waves, where all surface waves seem to overlay and run together. This Love wave-tunnel interference event should be particularly evident in the thick caliche overburden along the Mexican border.

The data was acquired with an 8-bit A/D instrument using 4 Hz horizontal geophones. The definition of weaker, higher frequency, scattered events, as compared to surface wave energies, requires better amplitude resolution. Moreover, higher frequency geophones would filter much of the low frequency, Love wave energy, thus giving more weight to the higher frequencies of the scattered events. While the results were good, they could have been even better with higher amplitude resolution instrumentation.

In conclusion, it is the opinion of the author that the test was successful and that the Love wave interference phenomena is the most probable procedure for successful detection of shallow tunnels located within unconsolidated surface materials.

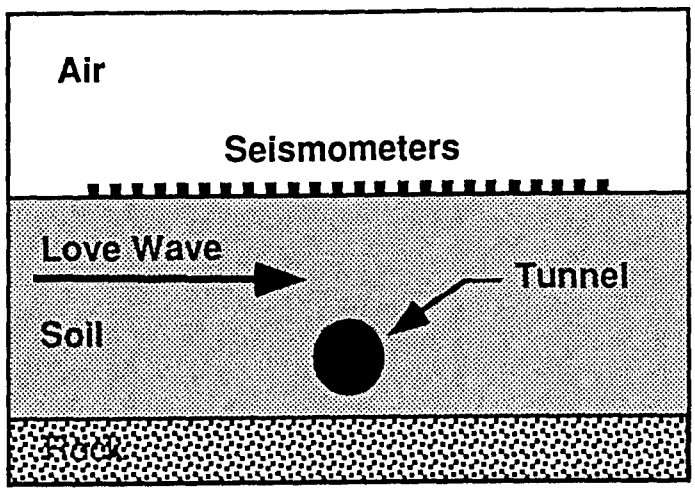

Figure 1a. Generic Tunnel Model

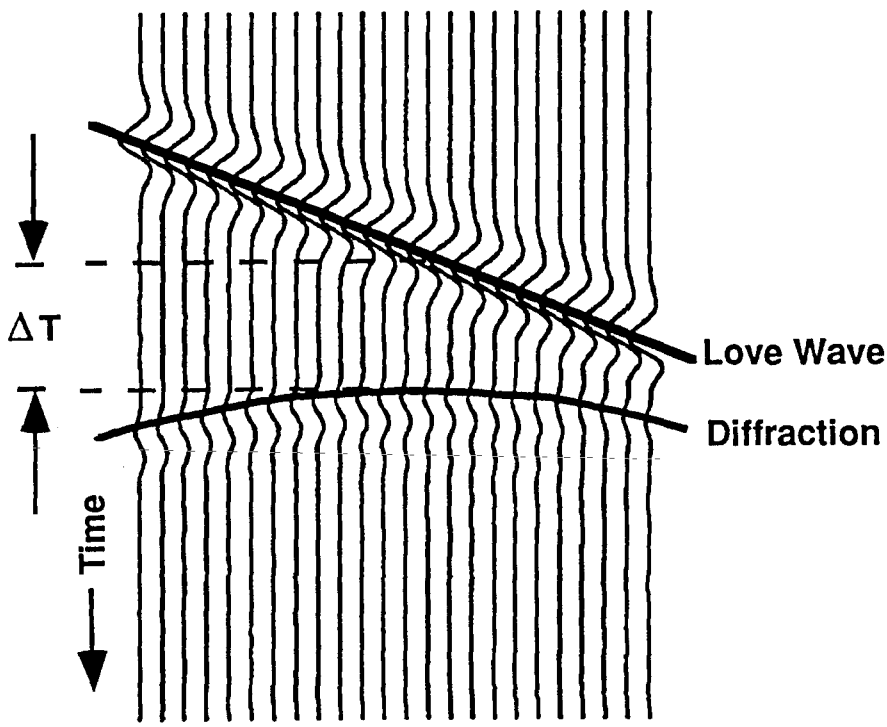

Figure 1b. Synthetic seismogram for Love wave-tunnel interaction.

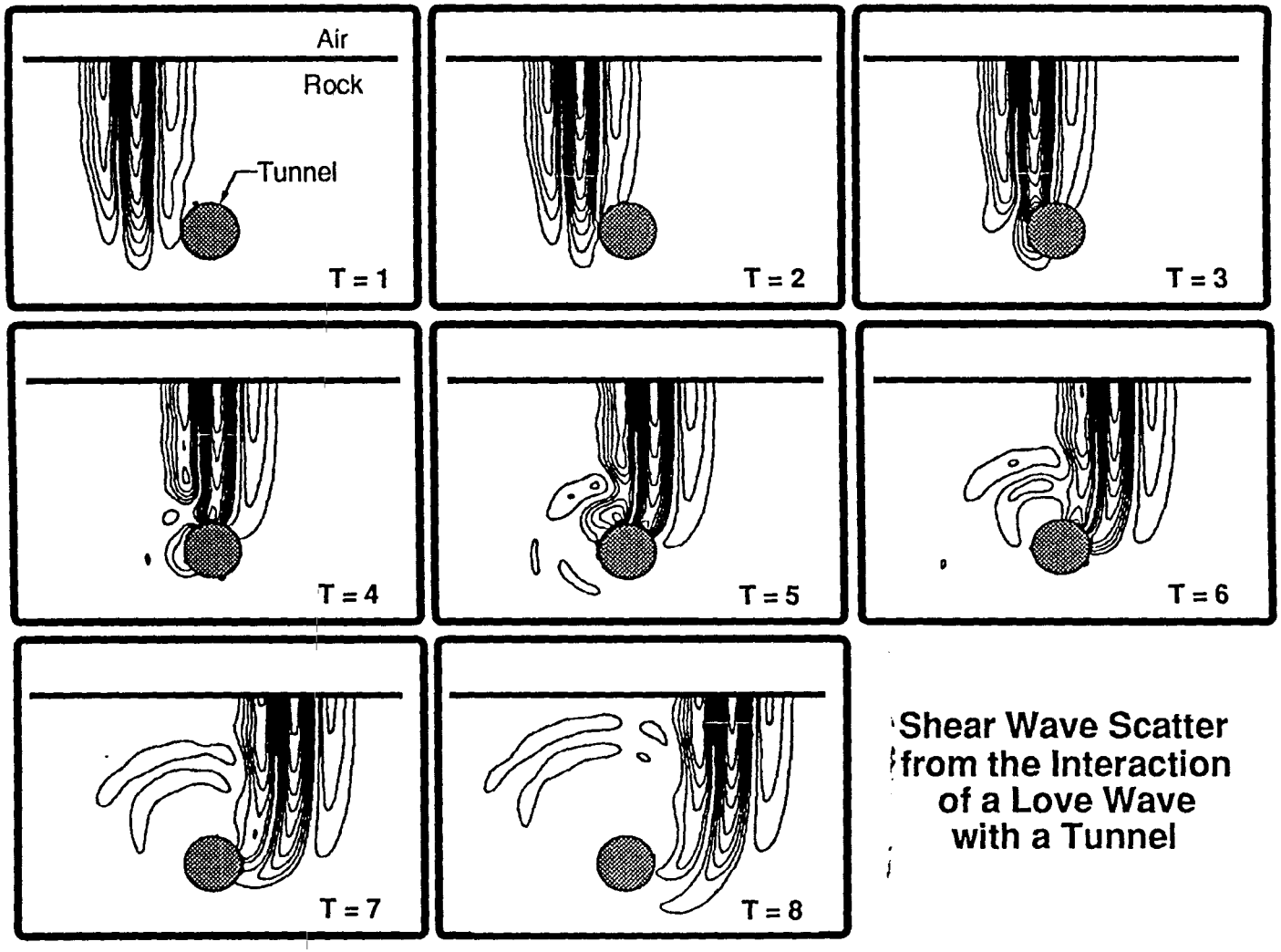

Figure 2. Time "snapshots".

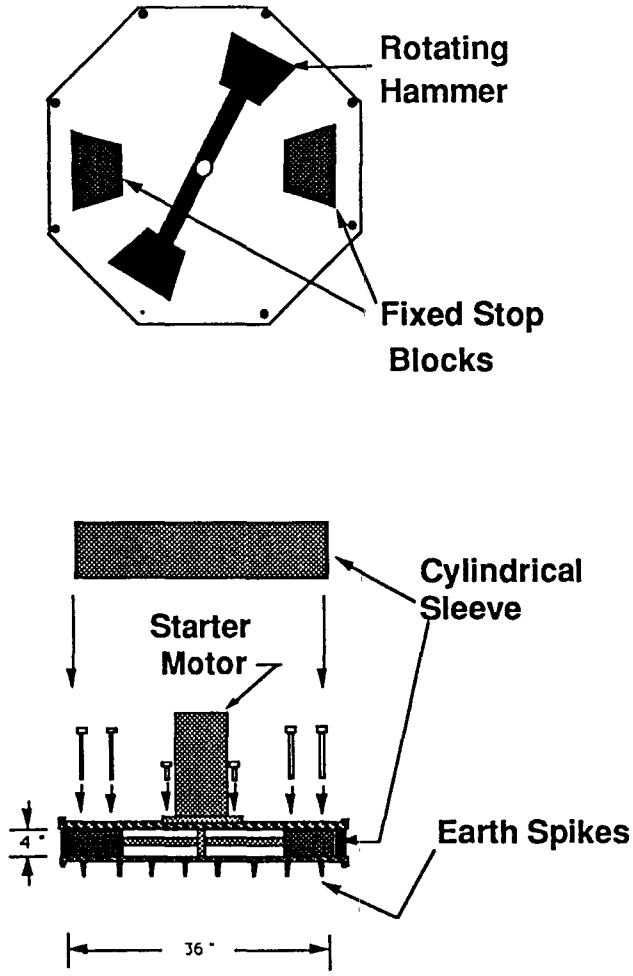

Figure 3a. Wacker schematic

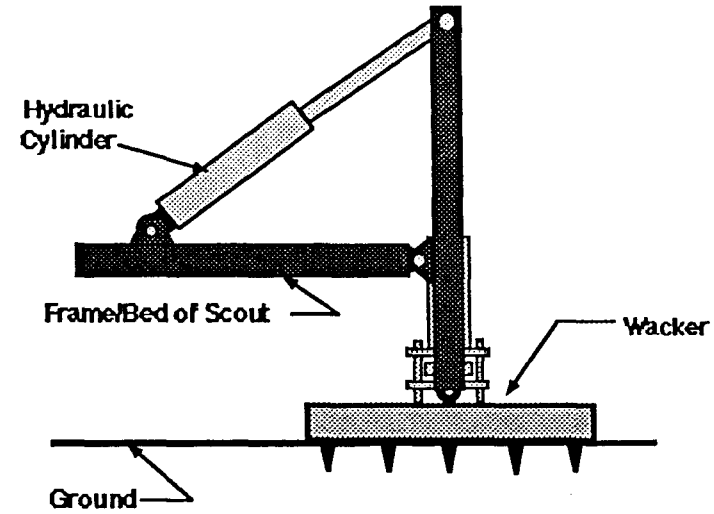

Figure 3b. Wacker Vehicle mount.

Figure 4. Wacker field deployment.

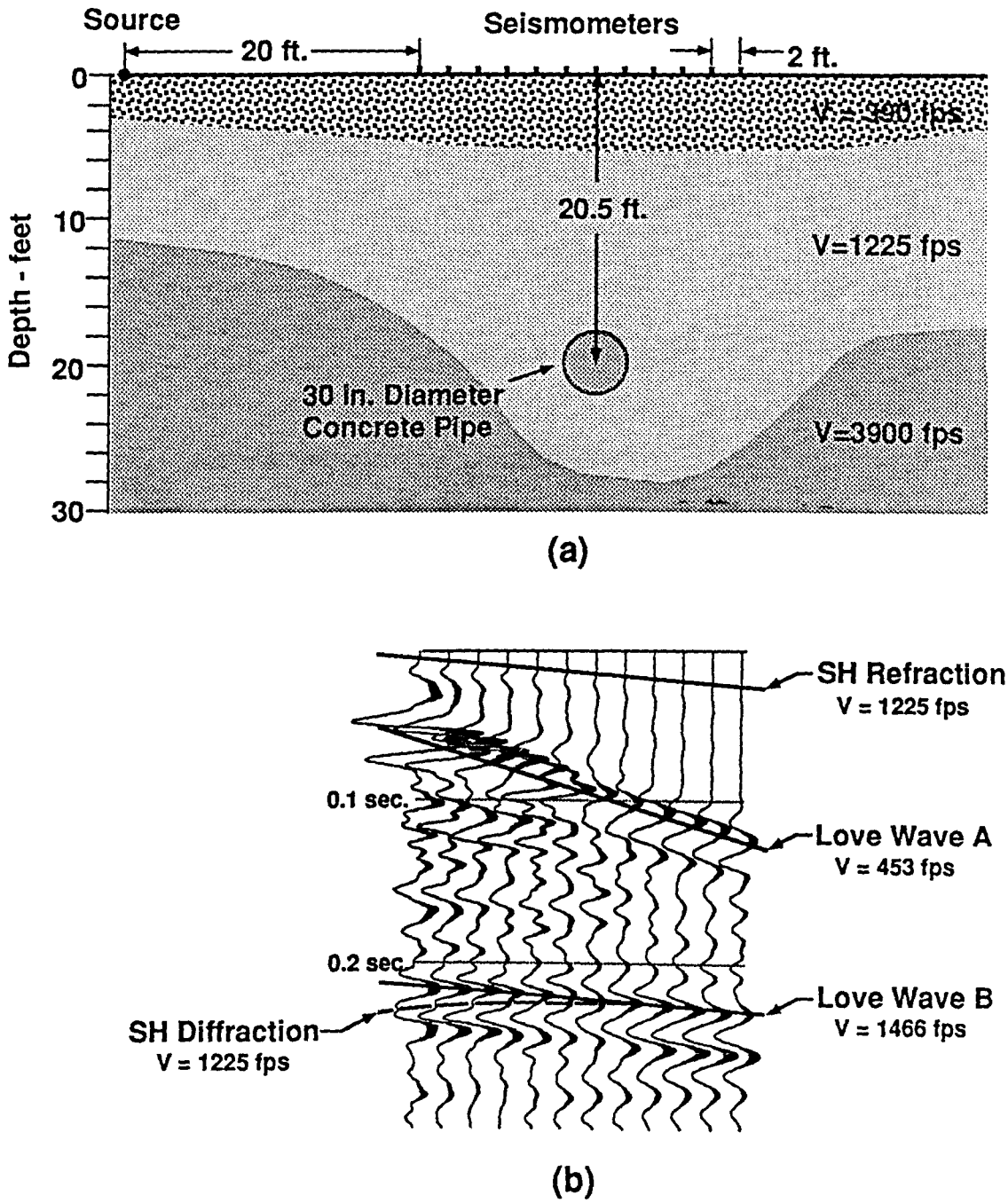

Figure 5. (a) Subsurface tunnel-host configuration as derived from refraction information. (b) SH seismogram for given source-sensor configuration.

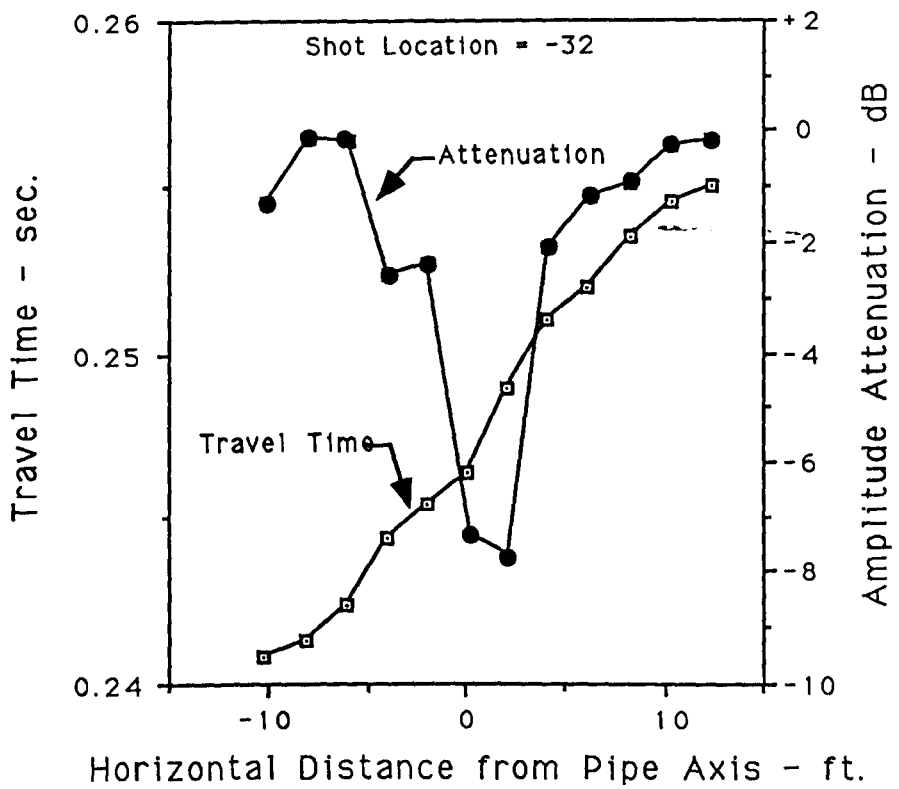

Figure 6. Love arrival time and attenuation.

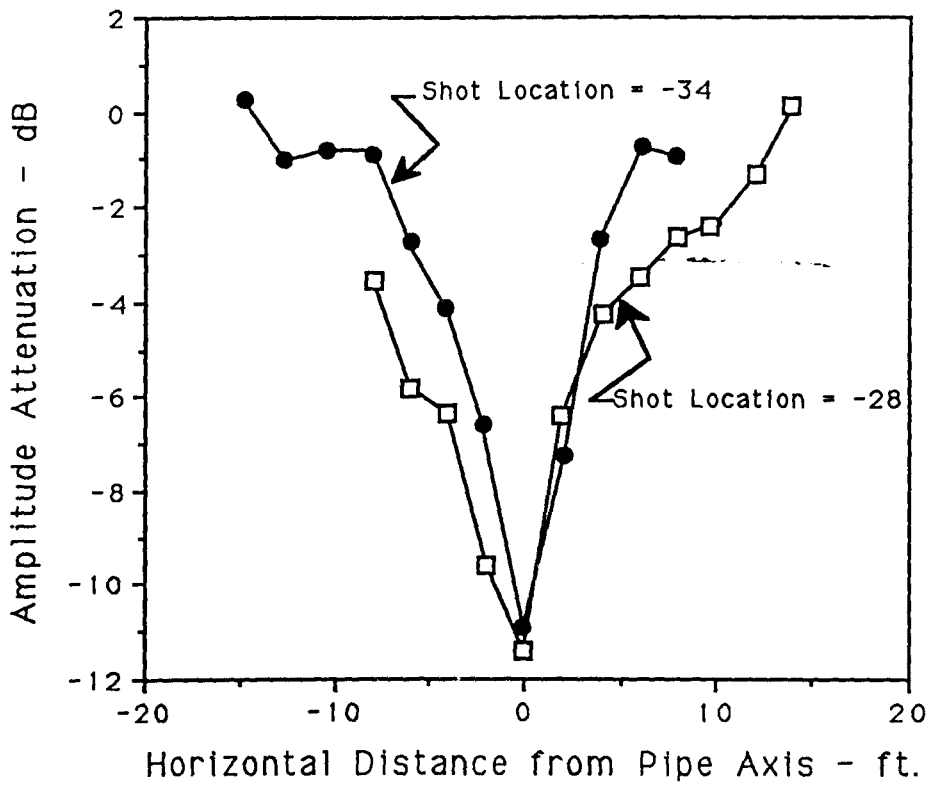

Figure 7. Love wave amplitude attenuation due to scattering.